

A critical overview of geophysical investigation and laboratory test results used in the seismic re-evaluation of the Farneto del Principe dam in Italy

Gianluca Regina

University of Calabria, Department of Civil Engineering, Arcavacata di Rende (CS), Italy,
gianluca.regina@unical.it

Ernesto Ausilio¹, Giovanni Dente²

University of Calabria, Department of Civil Engineering, Arcavacata di Rende (CS), Italy,
ernesto.ausilio@unical.it, giovanni.dente@unical.it

Paolo Zimmaro

University of California, Department of Civil and Environmental Engineering, Los Angeles,
pzimmaro@ucla.edu

ABSTRACT: This paper describes a comprehensive geotechnical characterization campaign performed on a major zoned earth dam in Southern Italy (the Farneto del Principe dam), by means of field investigation and laboratory test. Results from these tests will be used to perform a seismic re-evaluation of the dam, to comply with the new standards issued by the Italian National Authority for Dams. A series of invasive (cross-hole and down-hole) and non-invasive (multichannel analysis of surface waves, MASW) geophysical tests, in addition to traditional geotechnical field tests, such as cone penetration tests and standard penetration tests were carried out to evaluate geotechnical characteristics of the dam, focusing on shear wave velocity (and shear modulus) profiles of the clay core and the shells. Several cyclic laboratory tests by means of resonant column tests were also performed on undisturbed specimens collected in the clay core of the dam. Such data formed the basis for developing a geotechnical model used to evaluate the seismic response of the dam. As expected, we observe that in the clay core and the shells of the Farneto del Principe dam, the small-strain shear modulus increases with depth following a non-linear trend. Such test results are then compared to existing empirical models. This study aims to provide insights into the geotechnical and geophysical characterization of existing dams. As such, it could be used as a benchmark for planning future field investigation campaign studies.

Keywords: earth dam; cross-hole; down-hole; MASW; geophysical tests

1. Introduction

Earth dams are essential infrastructures for the economy, our communities, and the society. Over the last century the global number of embankments rose almost exponentially [1], with Italy being no exception. Nowadays, most of the existing dams can be classified as “old structures”, as they have been in operation for decades. Thus, safety assessment of earth dams (under both static and dynamic conditions) is now becoming of great importance, particularly for dams suffering the effects of ageing. The geotechnical properties of the dam body materials may change over time (e.g. different grain size distribution in different zones of the dam – especially filters – due to seepage drag forces) and the current characteristics can be remarkably different from those estimated during the construction period. It has been shown [2] that under static conditions, damage to earth dams occurs immediately after the end of construction, or several years later. For these reasons, the analysis and monitoring of the dam must be performed periodically, to ensure the functionality of the structure.

The above considerations are particularly true for seismic performance evaluations, as the majority of earth dams in Italy were designed with old codes and/or standards that often accounted for the effects of

earthquakes only in a simplified manner. For instance, seismic load was typically represented as a pseudostatic force so only collapse due to mass sliding could be evaluated. However, several case histories [3-5] showed that there are many failure mechanisms and damage types related to dynamic action. During the past four decades, several investigators worked on the evaluation of the seismic response of earth dams [6-9]. This led to new methods of analysis, which can capture nonlinear behavior of soils, model the interaction between the dam and its foundation materials, and more faithfully reproduce the dynamic loading. As a result, the Italian National Authority for Dams has recently issued new standards and requested the seismic re-evaluation of all old earth dams in the Italian territory [10].

The aforementioned methods require a substantial computational effort and advanced numerical models (typically using large strain finite element or finite difference methods) based on the dynamic characteristics of the materials. Thus, a key component of seismic assessment of earth dams is represented by material characterization by means of field and laboratory tests.

In this paper, the results of a field and laboratory investigation campaign performed on a zoned earth dam in Southern Italy are presented. The investigations were conducted between 2015 and 2017. Details on the current static performance of this dam, along with some insights

from monitoring data are presented by Ausilio et al. [11, 12].

2. The Farneto del Principe dam

The Farneto del Principe dam is located in the town of Roggiano Gravina in Southern Italy (Latitude: 39.6515°N - Longitude: 16.1627°E). An overview of the dam is reported in Fig. 1. The dam is located in a seismically active region characterized by shallow crustal and deep seismicity. The latter is related to the subduction zone of the Calabrian arc [13]. The dam was designed at the beginning of the '60s and built between the late '70s and '80s. It is used for irrigation purposes and flow balancing. The dam height is 30 m and its length is more than 1200 m. The crest elevation is at 144.20 m above sea level (a.s.l.), the maximum authorized water surface level is 136.30 m a.s.l., and the maximum allowable level of the reservoir is 141.70 m a.s.l. The shells are composed of compacted sand and gravel, while the core is made up of compacted, low permeability clay and silt. Two filters (with a thickness of one meter each) protect the dam core. They are formed by sand on the core side and by sand and gravel on the shells sides. The dam is founded on alluvial materials (high permeability sands and gravels) which in turn overlay a deep clay bed. The thickness of the foundation materials is not constant but varies lengthwise, with a maximum thickness of around 43 m in the central area. A cut-off wall is present throughout the length of the dam, to prevent under-seepage. The cut-off wall was realized using two construction strategies: (1) two slurry walls formed by panels excavated in presence of the bentonite mud, and (2) a double line of close piles with half-meter diameter, without injection of waterproof material. The cut-off wall is embedded for 3 m into the clay bed for the whole longitudinal extension of the dam. Downstream the core is located an inspection gallery also used as a conduit for the collection of the drained water coming from the dam. A representative cross section is illustrated in Fig. 2. The main geometrical characteristics of the dam are reported in Table 1.



Figure 1. Overview of the Farneto del Principe dam.

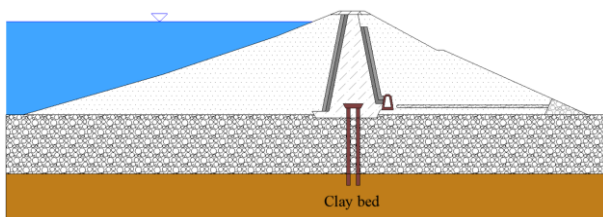


Figure 2. Schematic cross section of the Farneto del Principe dam

During the design and construction phases, a series of laboratory tests, such as oedometric, grain size

distribution, direct shear, and triaxial tests were performed on the soil used to build the dam. A summary of the main geotechnical parameters from these laboratory tests is reported in Table 2. Additional details on pre-construction tests and those performed during the construction of the dam is provided by Ausilio et al. [11, 12].

Table 1. Main geometrical characteristics of Farneto del Principe dam

| Geometrical property | Value |
|--|--------------------|
| Water storage volume | 46 Mm ³ |
| Average height (above the foundation) | 27.7 |
| Crest length | 1240 m |
| Crest width | 7 m |
| Freeboard (max level of the reservoir) | 2.7 m |
| Current freeboard | 8.1 m |
| Upstream face slopes | 1:2.5, 1:3, 1:3.5 |
| Downstream face slopes | 1:1.185, 1:2.25 |
| Crest elevation | 144.20 m a.s.l. |
| Maximum allowable water level | 141.70 m a.s.l. |
| Maximum authorized water level | 136.30 m a.s.l. |

Table 2. Geotechnical properties of the dam material.

| Parameter | Mean value | | |
|---|--------------------|----------------------|--------------------|
| | Alluvium | Core | Shells |
| Cohesion (kPa) | 0 | 80 | 0 |
| Friction angle (°) | 37.5 | 18 | 40 |
| Undrained strength (kPa) | - | 202 | - |
| Unit weight (kN/m ³) | 24.1 | 21.3 | 25.1 |
| Dry unit weight (kN/m ³) | - | 18.1 | 24.0 |
| Particle unit weight (kN/m ³) | - | 27.3 | 27 |
| Porosity | - | 0.338 | 0.110 |
| Void ratio | - | 0.510 | 0.123 |
| Degree of saturation (%) | - | 95.6 | 96.7 |
| Plasticity index | - | 26.16 | - |
| Water content (%) | 7.50 | 17.88 | 4.42 |
| Liquid limit (%) | - | 45.40 | - |
| Plastic limit (%) | - | 19.18 | - |
| Hydraulic conductivity (m/s) | 1x10 ⁻⁵ | 1.3x10 ⁻⁹ | 1x10 ⁻⁵ |

3. The 2015-2017 geotechnical investigation campaign

The available data on the dam material characterization should be complemented by new data. There are two main reasons for a new field investigation campaign: (1) some of the material properties may be different (e.g. grain size distribution changed over time in different zones); (2) several parameters are unknown (e.g. shear wave velocity profiles and modulus reduction and damping curves). The new geotechnical investigation campaign was specifically designed to fill these gaps. The field investigation campaign described in this study was carried out between 2015 and 2017. It comprises the following test types:

- a) Boreholes with continuous sampling;
- b) Standard Penetration Tests (SPT);

- c) Cone Penetration Tests with hydrostatic pore pressure evaluation (CPTu);
- d) Seismic Cone Penetration Tests (SCPTu);
- e) Seismic tomography;
- f) Down-hole and cross-hole tests;
- g) Multichannel Analysis of Surface Waves (MASW);
- h) Dynamic laboratory tests on undisturbed specimens (Resonant Column and Cyclic Torsional Shear tests);
- i) Microtremor Horizontal to Vertical Spectral Ratio (HVSr) analysis.

The locations of the aforementioned tests are reported in Fig. 3. Fifteen boreholes were drilled during the field investigation, eight on the dam crest, three on the landside shell, one near the guardhouse, one by the lateral overflow spillway, and two in the landside, in free field condition. For ten of the fifteen boreholes (S1, S2, S3, S4, S5, S6, S7, S8, S12, S13) SPTs were performed and five boreholes were equipped with Casagrande piezometers.

The perforations were executed using a Teredo MN 900 drilling rig, which operated with a rods system and a Shelby tube sampler (101 mm of internal diameter). This sampler is usually suitable for cohesive soils up to a firm-to-stiff consistency and free from large particles. As a result, a thick wall sampler with a core catcher was used to drill boreholes S2 and S3. The standard penetration tests (SPTs) have been performed following ASTM Standard procedures (D1586-11).

Two enhanced versions of the Cone Penetration Test (CPT) have been performed, namely piezocone tests (CPTu, with pore pressure measurement), and seismic CPT with piezocone (SCPTu, with seismic wave velocity measurement).

Eight seismic tomography have been performed. Five of them capture the two-dimensional distribution of shear wave velocity along longitudinal profiles: one is located along the crest, one near the guardhouse, two along the inspection gallery, and one in a free-field area on the landside of the dam. The remaining three tomographies are meant to characterize typical cross sections. One is located on the right bank (108 m long), one on the centerline (102 m long), and the last one on the left bank (96 m long).

Additional tests (down-hole, cross-hole, and MASW) were performed to define shear wave velocity profiles of various zones of the dam. Five down-hole tests were performed: in boreholes S3 (landside shell), S4 (crest), S13 (guardhouse), and S1 and S8 (the last two in a free field area). The S4 down-hole reached a depth of 26 m, investigating the clay core up until the cut-off wall. The S3 down-hole extended for 40 m, crossing both the dam shell and the alluvial foundations, while the S1, S8, and S13 reached the clay bed limit.

Four cross-hole tests were performed, using three boreholes (S4, S5, and S6 – these boreholes have an inter-boring spacing of four meters). Two tests were performed, utilizing two different source-receivers permutations (i.e. one time the source was in S4 and the receivers in S5 and S6, then source in S5 and receivers in S4 and S6). An inclinometer probe was used to ensure the verticality of the boreholes. The depth reached is 26 m, which is roughly the location of the concrete cut-off wall. The tests have been performed following the ASTM Standard procedures (D 4428).

A MASW test was also performed on the dam crest, using 24 4.5 Hz-geophones. The distance between the source and the first receiver was 5 m, while the inter-geophones spacing was 2 m.

Several dynamic laboratory tests on undisturbed specimens were also conducted on the dam crest materials (the specimens were collected in the following boreholes: S4, S5, S6, S11, and PZ3 following the ASTM Standard procedures, D 4015). Resonant Column (RC) and Cyclic Torsional Shear (CTS) tests were used to estimate the shear modulus of the clay core, its variation with depth, and its reduction with increasing shear strain. CTS tests were performed using a frequency of 0.1 Hz and various number of cycles (ranging from 5 to 20).

Microtremor Horizontal-to-Vertical Spectral Ratio (HVSr) analyses were also conducted on the dam crest, in a free-field area downstream of the dam, and in the inspection gallery. These tests were used to estimate the fundamental period of the dam. Data acquisition lengths ranged between 20 and 60 minutes. A portable Tromino 4 Hz seismometer with three receivers and a 24 bit digitizer was utilized. A summary of all tests performed is reported in Table 3.

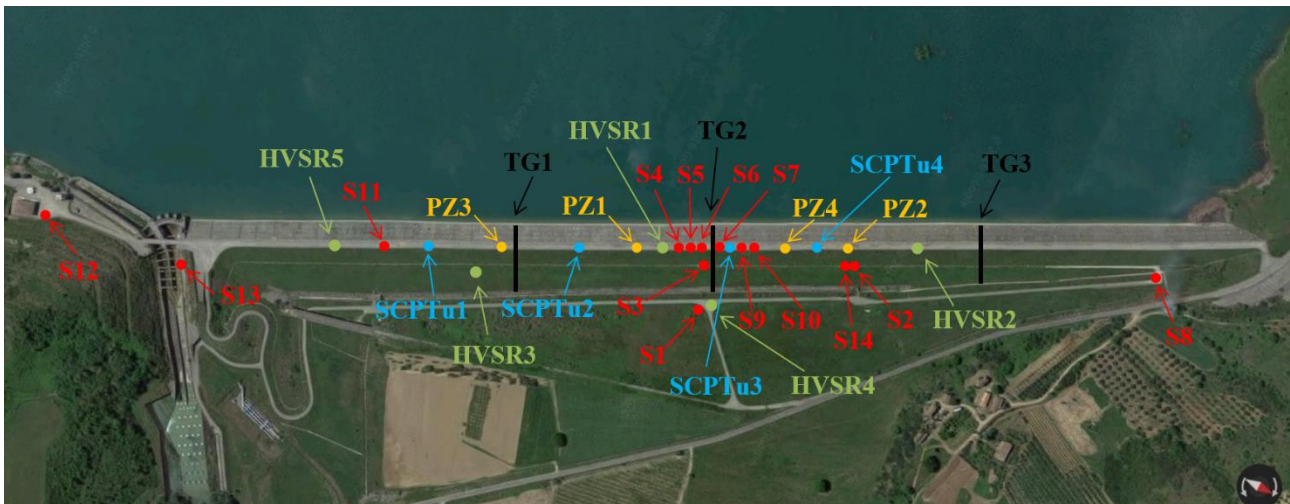


Figure 3. Locations of the tests performed at the Farneto del Principe dam.

Table 3. Summary of the tests performed at the Farneto del Principe dam site.

| Test type | Number | Location |
|------------------------|--------|---------------------------------------|
| Borehole | 15 | Core, shells, foundations |
| SPT | 10 | Core, shell, foundations |
| CPTu | 4 | Core |
| SCPTu | 4 | Core |
| Seismic tomography | 8 | Longitudinal and transversal profiles |
| Cross-hole | 4 | Core |
| Down-hole | 5 | Core, shell, foundations, guard house |
| MASW | 1 | Core |
| Resonant Column | 14 | Core |
| Cyclic Torsional Shear | 8 | Core |
| Microtremor HVSR | 5 | Core, inspection gallery, foundation |

4. Geophysical investigation and laboratory test results

The following sub-sections illustrate the results obtained from geophysical and laboratory tests. A critical analysis is carried out to explain the observed trends and compare measurements from this study with available data and empirical relationships in the literature. Differences between shear wave velocity profiles estimated using different tests are also highlighted and discussed.

4.1. Invasive geophysical tests

Four cross-hole tests, described in the previous section, were performed to estimate the shear wave velocity profiles at various locations within the dam core. The results are illustrated in Fig. 4. There is some scatter in the data obtained using different source-receivers permutations. This can be related to at least two reasons: (1) heterogeneity over a short length of the core material, and/or (2) poor cementation of the boring casings. The Authors consider the latter more pervasive since the material used to build the dam is believed to exhibit negligible longitudinal variability. Fig. 4 does not show results from a fourth cross-hole test, since its results are highly questionable, due to some issues in the data collection while in the field.

If analyzed holistically, the shear wave velocity profiles shown in Fig. 4 are somewhat consistent with previous studies [14, 15], where, for a homogeneous clayey material, a monotonic increase of the shear wave velocity with depth is expected. This is consistent with the notion that the shear modulus (and consequently the shear wave velocity) increases with increasing mean effective stress.

Down-hole tests were performed primarily to measure shear wave velocity profiles in the shells and in the alluvial foundations. A single test, however, was conducted inside borehole S4 (in the dam core), to

compare it with cross-hole and MASW results (sections 4.2 and 4.7).

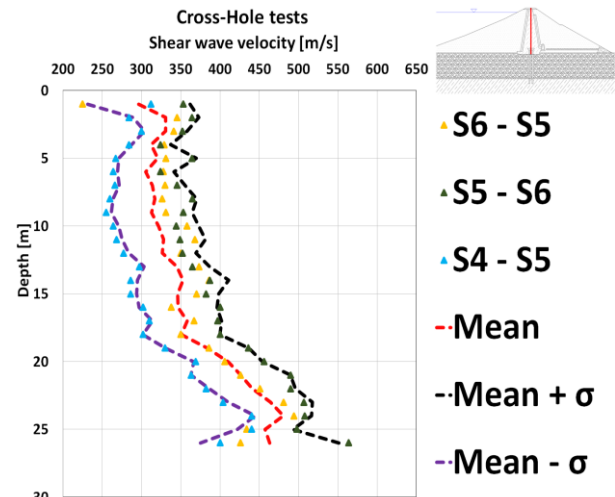


Figure 4. Shear wave velocity profiles in the dam core measured using cross-hole tests. The first ID in the legend is the location of the source, while the second is the location of the receiver.

Fig. 5 and 6 show shear wave velocity profiles at S1 and S8 (both in a free field area), measured by means of down-hole tests. These profiles are considered representative of the alluvial material on which the embankment is founded. The scatter in the data is related to the natural variability of this material and its intrinsic heterogeneity [16]. Furthermore, the thickness of this material varies longitudinally. As such, these two profiles cannot be directly compared.

Fig. 7 shows shear wave velocity profiles in the dam shell and in the alluvial foundation (boreholes S3 and S1 respectively). In both cases, the shear wave velocity increases with depth, reaching a maximum value of 700 m/s in the alluvial material (at the bottom of the test). However, for down-hole S3 there is a small discontinuity in the profile at the boundary between the shell material and the alluvial foundation material. This transition is less abrupt in the data from S1. It is interesting to compare the absolute value of the shear wave velocity of the alluvial foundation material measured beneath the shells and in the free field areas. Fig. 7 shows such comparison for down-holes S1 and S3. The shear wave velocity of the alluvial material beneath the dam is substantially higher than that in the free field area at the same elevation. In particular, it takes about 20 m for the shear wave velocity in the alluvial material in free field condition to reach the value measured in the same unit immediately beneath the dam. This comparison highlights the expected effect of overburden pressure on shear wave velocity profiles.

4.2. Multichannel Analysis of Surface Waves (MASW)

The Multichannel Analysis of Surface Waves is a non-invasive method to estimate shear wave velocity profiles. One such test has been performed on the dam crest to characterize the dam core. Fig. 8 illustrates the position of the receivers on the dam crest.

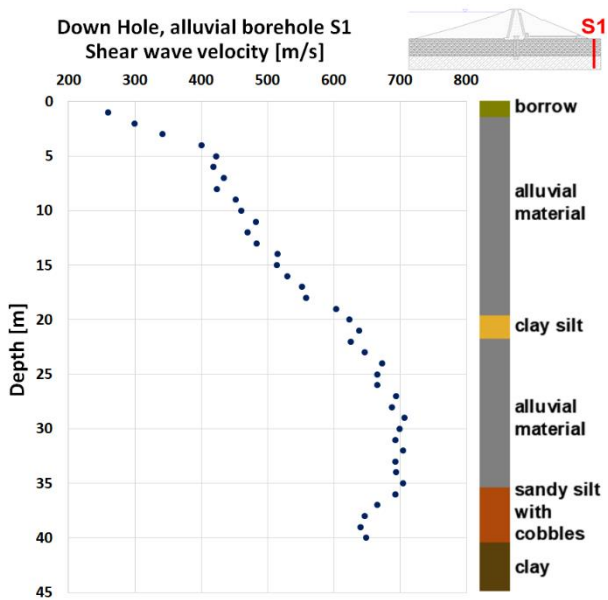


Figure 5. Shear wave velocities evaluated from down-hole test in a free field area. The location of the borehole S1 is at the center of the alluvial foundations.

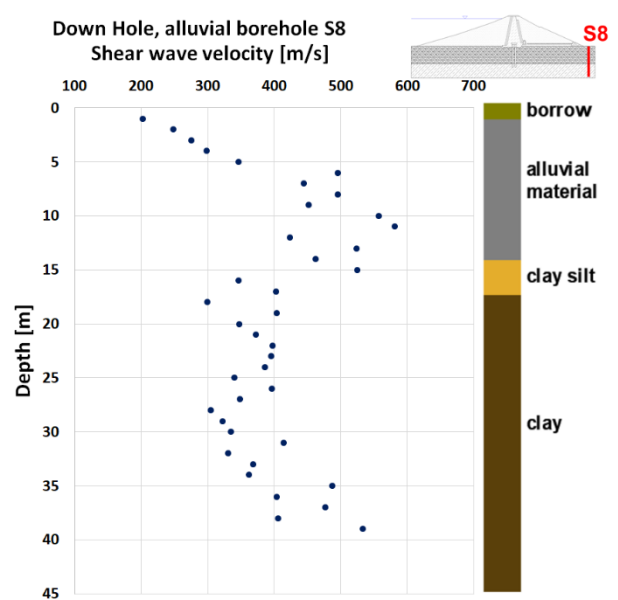


Figure 6. Shear wave velocities evaluated from down-hole test in a free field area. The location of the borehole S8 is at the left bank.

Fig. 9 shows the measured dispersion curve in terms of phase velocity versus frequency, while Fig. 10 shows one inverted profile. The profile of Fig. 10 represents one of the many potential inverted profiles. As a result, it carries a relatively high level of uncertainty. The inverted profile of Fig. 10 is generally consistent with the profiles obtained in the same materials using invasive tests. It shows an initial value of 320 m/s in the upper 2 m. This high value is representative of a 2m-thick sealing layer made of asphalt and concrete. After this layer, there is a visible inversion of the velocity profile, which then exhibits a trend of increasing velocity with depth. At a depth of 28m, the shear wave velocity value jumps to 700 m/s due to the presence of the concrete cut-off wall. Similar results were found for dams in Korea by Park and Kishida [15]. They observed that MASW results are in good agreement with invasive tests for depths up to 25 m in the clay core.

4.3. Microtremor HVSR analysis

The results obtained from microtremor HVSR analysis are illustrated in Fig. 11. The spectral ratio curves evaluated in free-field condition and in the inspection gallery are basically flat (Fig. 11a and 11b) indicating negligible impedance contrast in the soil profiles at these locations. This is consistent with the results of the down-hole S1. These curves capture the behavior of the alluvial material on which the dam is founded. Four HVSR curves are available for the dam crest (Fig. 11c-f). At the dam crest, the first spectral ratio peak (indicating the fundamental frequency of the structure) for all HVSR analyses, is in the frequency range 2-3 Hz (i.e. a period range 0.33-0.5s), while the second peak (indicating higher modes) is at frequencies between 4 and 5 Hz (i.e. a period range 0.2-0.25s).

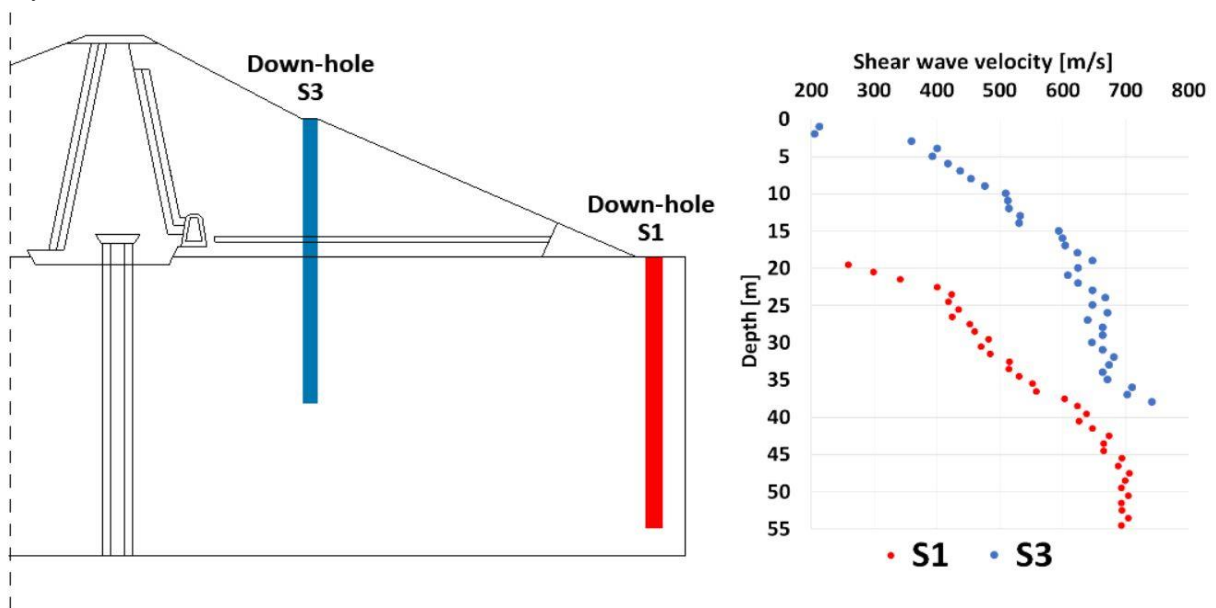


Figure 7. Shear wave velocities in the dam shell and in the alluvial foundations.



Figure 8. Execution of the MASW test and positions of the receivers.

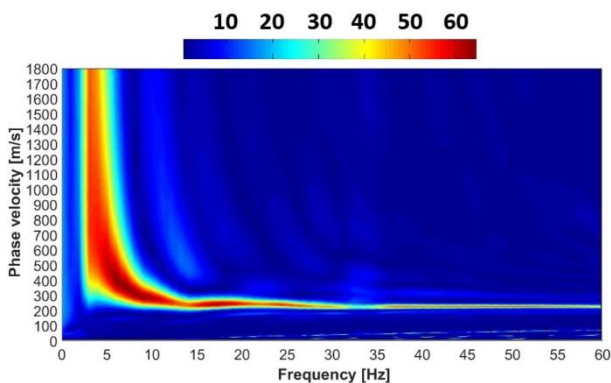


Figure 9. Dispersion curve obtained at the Farneto del Principe dam crest.

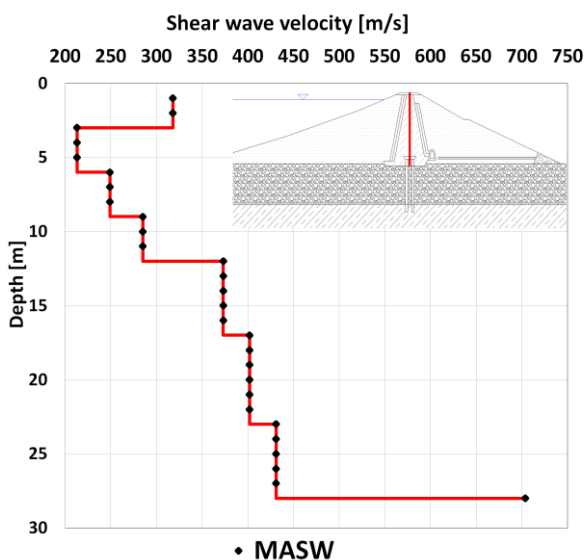


Figure 10. Inverted profile of shear wave velocity.

Zimmaro [17] performed a finite element method numerical modal analysis for this dam, estimating its fundamental period to be 0.25s. The results from the HVSR analysis presented here are roughly comparable to those provided by the numerical model. This is especially so if considering that the numerical model ignored the effects of the reservoir, utilized a different water level in the embankment, and was based on approximate geotechnical parameters. Fig. 12 shows the ratio of the E-W horizontal component measured at various locations,

divided by that measured in free-field conditions. This figure shows that the first peak measured at the dam crest is not present in the inspection gallery. This is a further confirmation that the fundamental frequency of the dam should be in the range 2-3 Hz, and that at 4-5 Hz the HVSR analysis shows a higher mode frequency. Similar conclusions can be drawn using the other horizontal component (N-S).

4.4. Seismic tomography

Results from seismic tomographies are useful to identify general trends of seismic waves velocities within the embankment. Furthermore, such tests can help identifying heterogeneities in the construction materials. The results of two transversal tomographies are illustrated in Fig. 13. Results from these seismic tomographies do not show an evident stiffness contrast between the dam materials (core and shells) and the alluvial foundation present in the foundation. However, a shallow layer with low seismic wave velocity can be identified on both the upstream and downstream face of the dam, which indicates a low compaction level near the surface. This result is consistent with other tests (i.e. MASW) performed on the dam materials.

Fig. 14 shows the result of the seismic tomography for the longitudinal profile of the dam (performed on the dam crest). The profile is around 700 m long and shows a remarkable stiffness contrast between the dam body and the alluvial material. The clay bed shows velocities slightly higher than the alluvial materials, although the stiffness contrast is not dramatic. These results are not consistent with what can be observed looking at the down-hole performed in boring S8. This may be a proof of the spatial variability of the alluvial foundation.

4.5. Laboratory test results

Resonant column and Cyclic Torsional Shear tests were used to evaluate the dynamic properties of the dam core material (i.e. shear modulus reduction and damping curves). Shear wave velocity of the specimens were also estimated based on the small strain shear modulus and the results are shown in Fig. 15.

Shear wave velocities estimated from CTS are 10% smaller compared to RC results. This is expected, as RC tests are conducted at high frequencies, which leads to a higher shear modulus and consequently shear wave velocity [18]. The trend of increasing velocity with depth shown by field investigation data is captured by both laboratory tests.

Shear modulus reduction and damping curves are shown in Fig. 16, along with the mean curves fitting the data. The shear modulus reduction values are relatively constrained in a narrow range, while damping values are more scattered. These tests were performed on specimens taken at different depths (i.e. from 3 to 21 m, with a 3 m interval). However, this data does not show an evident overburned stress effect on the modulus reduction and damping curves. Thus, while the small strain shear modulus does increase with depth, the variation with distortional strain is basically the same.

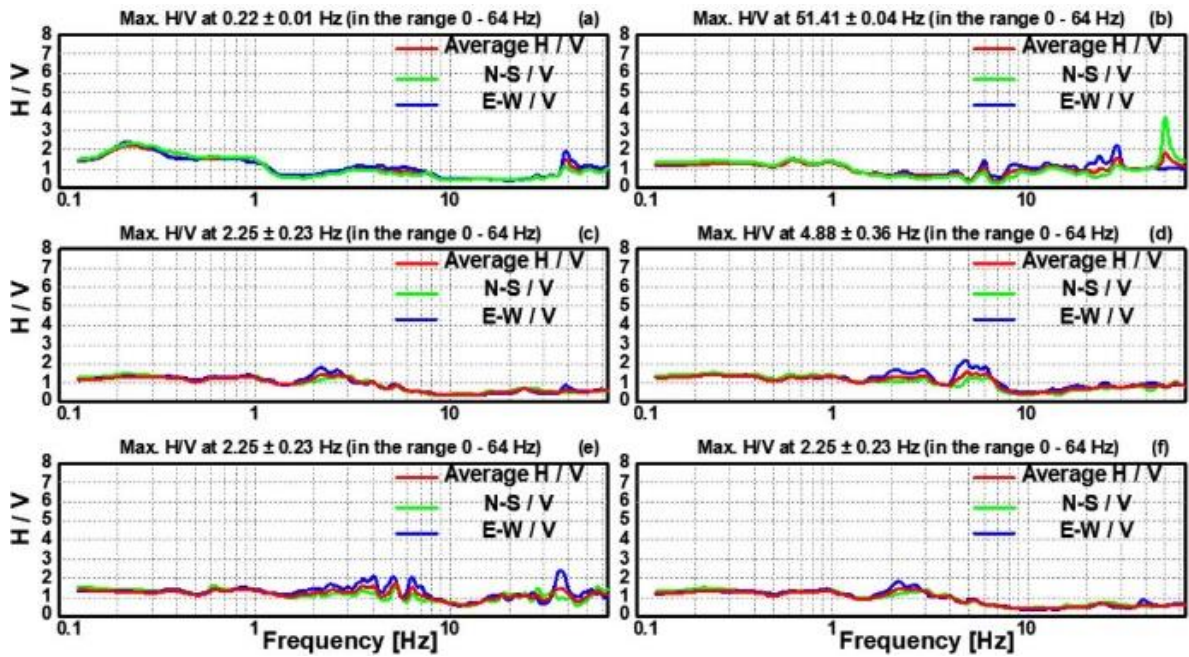


Figure 11. Microtremor HVSR results: (a) free field area; (b) inspection gallery; (c),(d),(e), and (f), dam crest.

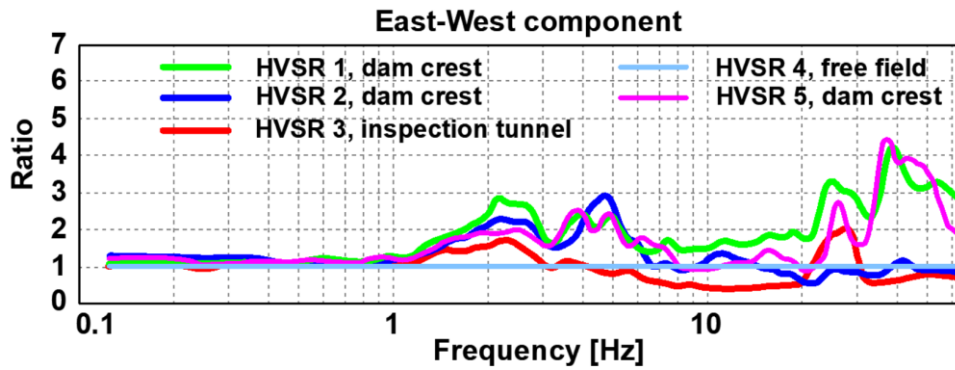


Figure 12. Ratio of the microtremor E-W horizontal component measured at various locations, divided by that measured in free-field conditions.

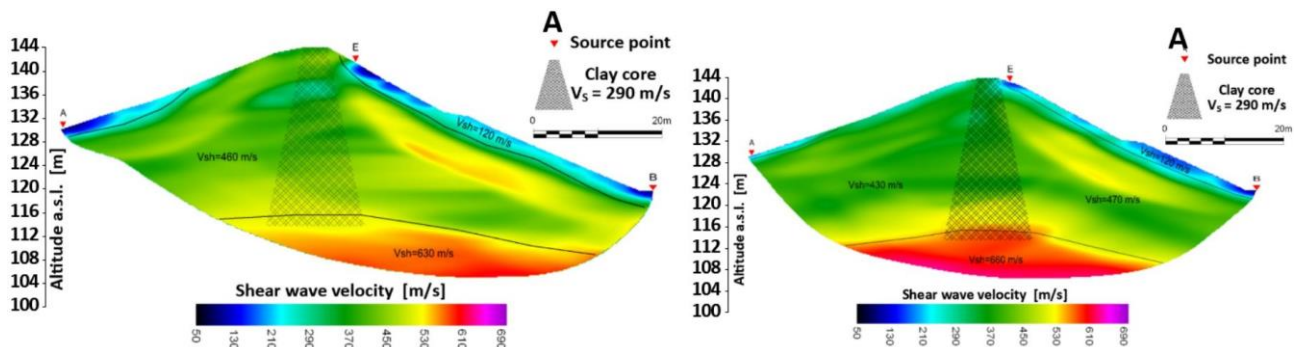


Figure 13. Transversal profile of shear wave velocity evaluated from seismic tomography performed at the Farneto del Principe dam.

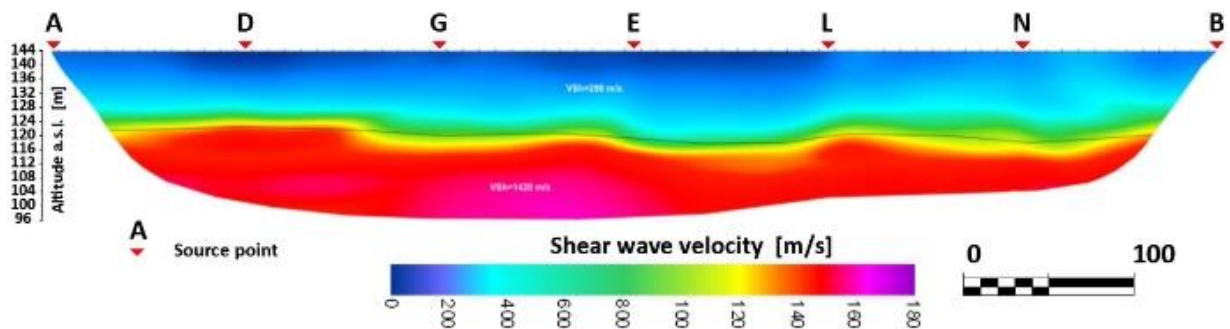


Figure 14. Longitudinal profile shear wave velocity evaluated from seismic tomography performed at the Farneto del Principe dam.

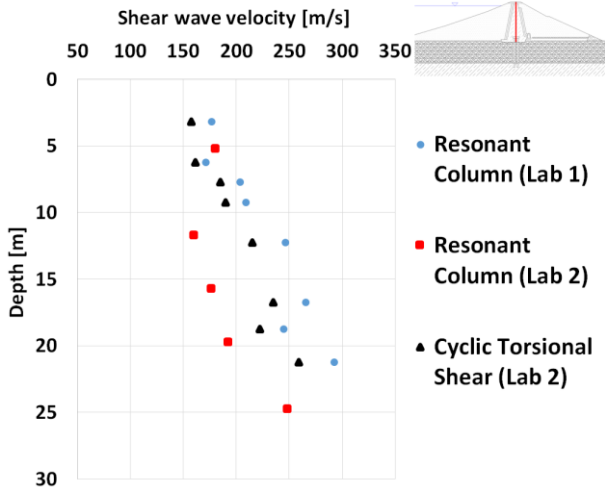


Figure 15. Shear wave velocities estimated from laboratory tests with undisturbed specimens.

The shear modulus reduction and damping curves obtained at the Farneto del Principe dam and those presented by Kishida and Park [19], who analyzed 28 earth dams in Korea, are different from the classical curves of Vucetic and Dobry [20]. This is expected, because the dam clay core is made up of compacted material, while the Vucetic and Dobry curves were derived from materials representative of natural soil. In Fig. 16 the Vucetic and Dobry curves for a Plasticity Index of 26 (the mean value in the dam core) are reported. The Farneto del Principe shear modulus reduction curves show that the dam core material has an apparent linear behavior up to shear strain of 0.01%, with a strong non linear trend afterwards. This material is more linear than what it would be predicted using the curve by Vucetic and Dobry [20]. The shape of the mean damping ratio curve is different than that presented by Vucetic and Dobry [20], as small-strain damping values of earth core materials are typically higher than those of natural soils [19].

4.6. Shear wave velocity from correlations

Four SCPT were performed on the dam crest, to evaluate the mechanical properties and the mean shear wave velocity value. The results are reported in Fig. 17.

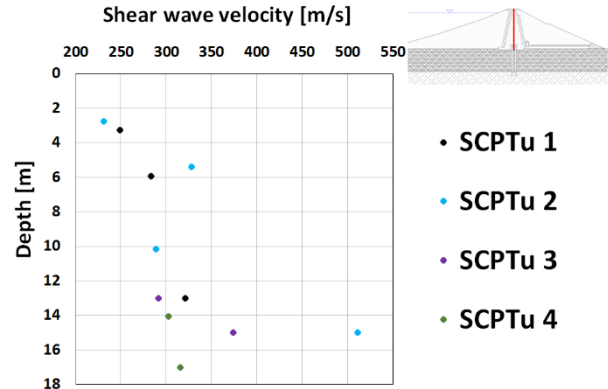


Figure 17. Shear wave velocity estimated from SCPTu tests.

In addition to them, four standard CPTs were also performed. Using data from these CPTs, shear wave velocity profiles can be estimated using empirical correlations.

Such relationships relate the cone tip resistance (q_c) and sleeve friction (f_s) with shear wave velocity values. They are typically locally applicable and usable for specific soil types. The following expressions were used in this study:

- Mayne and Rix [21]

This relationship is valid for intact and fissured clays in a huge range of plasticity index (PI), sensitivities (S_t), and overconsolidation ratio (OCR) ($8 < PI < 300$, $2 < S_t < 200+$, and $1 < OCR < 100+$). The data are referred to 31 sites from all around the world:

$$V_S = 1.75 q_c^{0.627} \quad (1)$$

where q_c is expressed in kPa and the shear wave velocity (V_S) in m/s.

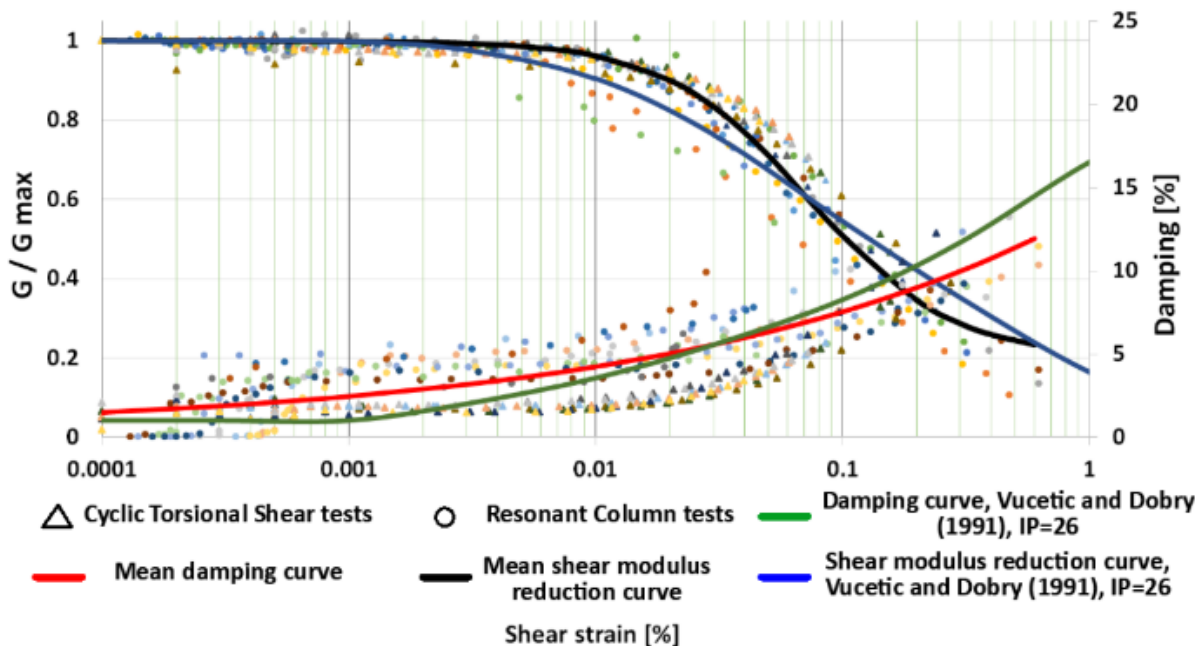


Figure 16. Shear modulus reduction and damping curves for the Farneto del Principe dam clay core.

- Hegazy and Mayne [22]

This expression is valid for clays and it is an updated version of Eq. (1):

$$V_S = 3.18 q_c^{0.549} f_s^{0.025} \quad (2)$$

where q_c and f_s are expressed in kPa and V_S in m/s.

- Piratheepan [23]

The relationship uses data from Canada, Japan, and the Unites States of America and it is valid for clays:

$$V_S = 11.9 q_c^{0.269} f_s^{0.108} D^{0.127} \quad (3)$$

where D is the depth measurement in meter and q_c and f_s are expressed in kPa.

- Mayne [24]

The relationship was developed from CPT data from various sites worldwide:

$$V_S = 118.8 \log f_s + 18.5 \quad (4)$$

where f_s is express in kPa and V_S in m/s. Equation (4) is presented in the form recommended by [25] with V_S as a function of the logarithm of f_s , rather than the natural logarithm as originally proposed in [24, 26].

The results are illustrated in Fig. 18. While the trend of increasing shear wave velocity with depth seems to be captured, the actual estimated values are generally lower than those measured by means of geophysical tests and presented above. Fig. 18 also shows a large scatter in the profiles estimated using empirical models.

Shear wave velocity values can also be estimated using SPT data. In this study, the following relationships were used:

- Otha and Goto [27]

This equation is based on data from alluvial plains in Japan. For clays, the authors suggest that the shear wave velocity value can be estimated as:

$$V_S = 68.79 N_{SPT}^{0.171} z^{0.199} f_a f_g \quad (5)$$

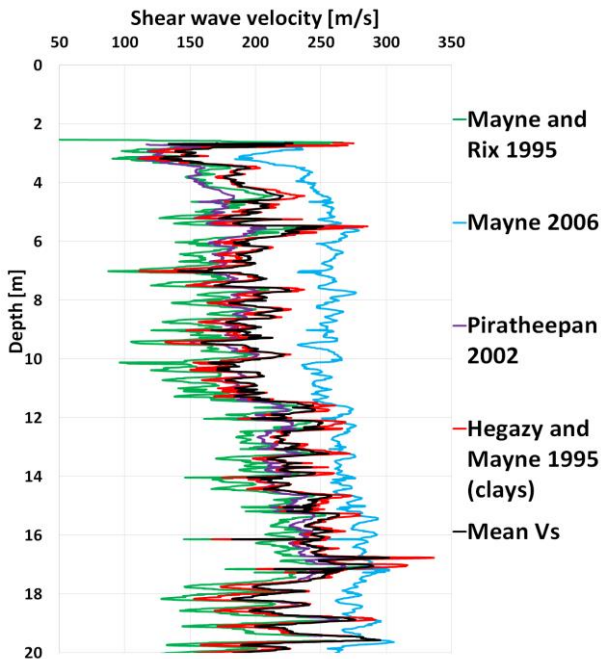


Figure 18. Shear wave velocity estimated from empirical relationships. The data refer to the mean of the eight CPT tests performed on the dam crest

where N_{SPT} is the blow count, z is the depth, f_a is a coefficient related to the geological age of the soil, and f_g is a coefficient based on the grain size distribution.

- Lee [28]

The relationship uses the N_{SPT} value corrected for energy efficiency and overburden stress (N_{160}). This relationship is based on data from Taiwan.

$$V_S = 131.7 (N_{160} + 1.2)^{0.31} \quad (6)$$

- Athanasopoulos [29]

$$V_S = 76.55 N_{SPT}^{0.445} \quad (7)$$

- Pitilakis et al. [30]

The authors give correlation equations for clays, silts, and sands, based on geophysical measurements at the EURO-SEISTEST test site, in Greece.

$$V_S = 132 N_{160}^{0.271} \quad (8)$$

- Jafari et al.[31]

$$V_S = 27 N_{SPT}^{0.73} \quad (9)$$

- Petrangeli et al. [32]

This relationship is based on several data from Italy.

$$V_S = \alpha + \beta_1 N_{SPT} \quad (10)$$

where α and β_1 are parameters that depend on the soil type. Fig. 19 shows that the estimated shear wave velocity values are generally higher compared to those obtained from CPT relationships, but still lower than those measured by means of geophysical tests. A summary of the empirical relationships used in this study is provided in Table 4.

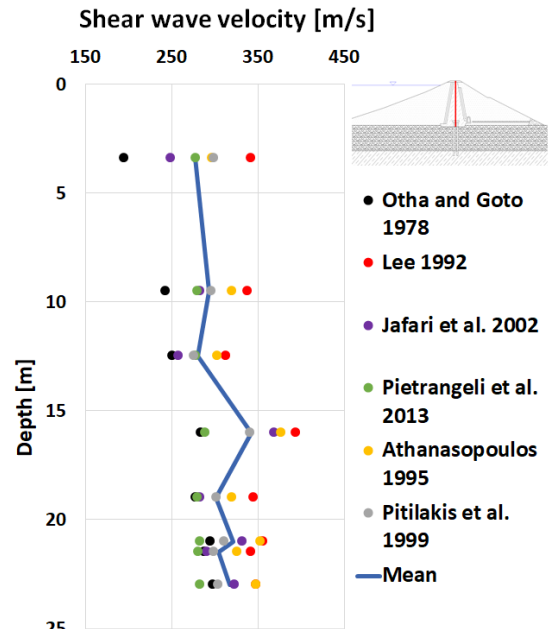


Figure 19. Shear wave velocity estimated from empirical relationships. The data refer to the mean of the four SPT tests performed on the dam crest.

4.7. Discussion

Fig. 20 shows a summary of all the shear wave profiles measured and estimated using empirical relationships. The expected trend of increasing shear wave velocity

with depth is captured by all tests. This between-method consistency may be an indication of the fact that the in-situ measurements were performed properly.

The velocities estimated from empirical relationships are generally lower than those measured with direct tests. This is a well-known issue related to these correlations [26].

Table 4. Empirical relationships used to estimate the shear wave velocity from in situ tests

| Relationship | Test | Expression |
|------------------------|------|---|
| Mayne and Rix 1995 | CPT | $V_S = 1.75 q_c^{0.627}$ |
| Hegazy and Mayne 1995 | CPT | $V_S = 3.18 q_c^{0.549} f_s^{0.025}$ |
| Piratheepan 2002 | CPT | $V_S = 11.9 q_c^{0.269} f_s^{0.108} D^{0.127}$ |
| Mayne 2006 | CPT | $V_S = 118.8 \log f_s + 18.5$ |
| Otha and Goto 1978 | SPT | $V_S = 68.79 N_{SPT}^{0.171} z^{0.199} f_a f_g$ |
| Lee 1992 | SPT | $V_S = 131.7 (N_{1,60} + 1.2)^{0.31}$ |
| Jafari et al. 2002 | SPT | $V_S = 27 N_{SPT}^{0.73}$ |
| Piترangeli et al. 2013 | SPT | $V_S = \alpha + \beta_1 N_{SPT}$ |
| Athanasopoulos 1995 | SPT | $V_S = 76.55 N_{SPT}^{0.445}$ |
| Pitilakis et al. 1999 | SPT | $V_S = 132 N_{1,60}^{0.271}$ |

The shear modulus (G) can be easily calculated from shear wave velocity values. In this study, it is compared to the well-known relationship by Dakoulas and Gazetas for homogeneous dams [33]. The authors provided the following expression:

$$G(z) = G_b \left(\frac{z}{H}\right)^m \quad (11)$$

where G_b is the shear modulus at the base of the core, H is the dam height, and m is the inhomogeneity factor which depends on the material, geometry, and relative stiffness of the core (its value is usually in the range of 0.3 – 0.8). A representative schematic of the shear modulus profile within a dam body obtained using this expression is depicted in Fig. 21, while further details are available in [33, 34].

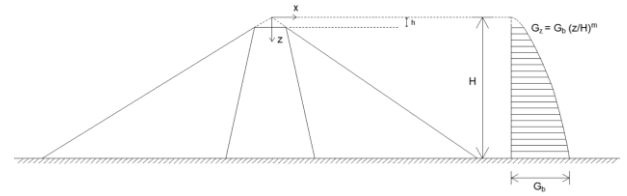


Figure 21. Shear modulus profile in a homogeneous dam according to Dakoulas and Gazetas [33]

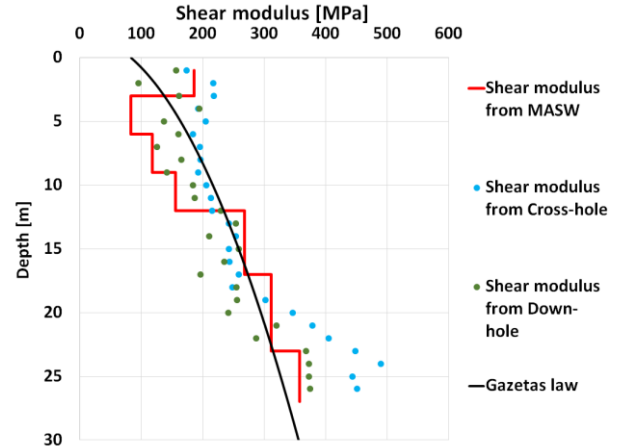


Figure 22. Gazetas law for predicting the shear modulus variation in the dam core. The curve is fitted based on the cross-hole, down-hole, and MASW results.

Fig. 22 shows a comparison between the shear modulus calculated for the Farneto del Principe dam using in-situ tests and the same value as obtained using the expression provided by Dakoulas and Gazetas [33]. It appears that the analytical expression of Eq. 11 fits the data reasonably well. In this comparison the value of the inhomogeneity factor is 0.5.

5. Conclusions

In this paper the results of a comprehensive geotechnical investigation campaign performed on a zoned earth dam in Southern Italy is presented. The Farneto del Principe dam is located in a highly seismic area, thus a re-evaluation of the performance under dynamic loading is necessary. Such assessment, however, requires the use of advanced methods of analysis that need several input parameters. These physical quantities (e.g. shear wave velocity and shear modulus reduction curves) can only be determined with an extensive field investigation, using appropriate in-situ and laboratory tests.

Three cross-holes, one down-hole, and one MASW were performed on the dam crest to estimate the shear wave velocity profile in the clay core. The results provided by these geophysical tests are in a good agreement and show a trend of increasing shear wave velocity with depth. Such trend is also confirmed by a MASW test. A cross-hole test, however, was not deemed representative, as the data were scattered and inconsistent with other tests. There is also some variability between the values reported in Fig. 4; this is probably due to a relatively poor cementation of the PVC pipes and the adjacent soil. While it is true that cross-hole tests usually provide a good level of accuracy, this is only valid when the test is perfectly executed.

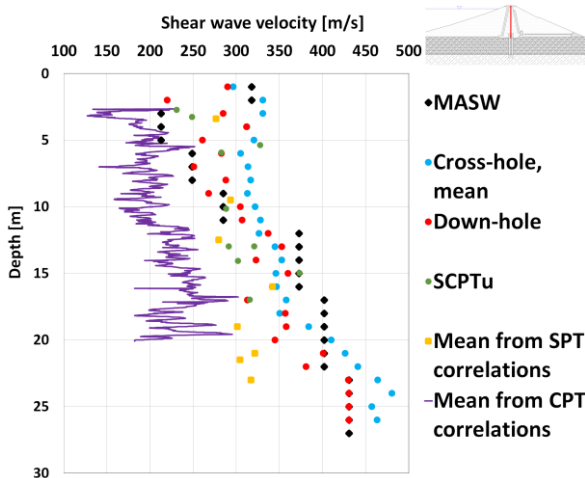


Figure 20. Comparison of shear wave velocity in the dam core estimated from geophysical tests and empirical relationships.

The down-hole tests performed on the downstream shell and alluvial foundations show, as expected, the influence of the overburden stress on the shear wave velocity. Furthermore, it shows some spatial variability in the alluvium, highlighting the need to carry out more geophysical tests when the site has a complex geological structure and potentially variable geotechnical characteristics.

A series of empirical relationships to estimate shear wave velocity profiles from CPT and SPT data were analyzed. These relationships are strictly valid only for specific soil types and are typically locally applicable. However, this study shows that they can capture the trend of shear wave velocity with depth, while generally underestimating the actual value of this quantity. It is suggested to treat such relationship with care, especially when they are applied to earth dams.

Several laboratory tests were also performed to evaluate the dynamic properties of the dam core. The results in this study show that the mean confining stress does not have a strong effect on the dynamic properties of this material. This conclusion is structure-specific, as the moderate height of this dam did not provide a large range of confining pressures. For this dam, shear modulus reduction curves are generally higher than those available in the literature for natural clays and the clay materials of this dam are more linear than what it would be predicted using empirical relationships. This is likely due to the effect of the material compaction during the construction of the dam.

Seismic tomography and HVSR were also performed. These tests were conducted before the invasive tests, to provide a general idea on the overall shear wave velocity trends. The aforementioned results will be used to evaluate the seismic performance of the Farneto del Principe dam.

6. References

- [1] Penman, A. D. M. "On the embankment dam", *Geotechnique*, 36, pp. 301–348, 1986. <https://doi.org/10.1680/geot.1986.36.3.303>.
- [2] Foster, M., Fell, R., Spannagle, M. "The statistics of embankment dam failures and accidents", *Canadian Geotechnical Journal*, 37, pp. 1000–1024., 2000. <https://doi.org/10.1139/t00-030>
- [3] Seed, H. B., Lee, K. L., Idriss, I. M., Makdisi, F. I. "The slides in the San Fernando Dams during the earthquake of February 9, 1971", *Journal of Geotechnical and Geoenvironmental Engineering*, 101, pp. 651–688, 1975.
- [4] Seed, H. B., Lee, K. L., Idriss, I. M. "Analysis of Sheffield Dam Failure", *Journal of the Soil Mechanics and Foundations Division*, 95, pp. 1453–1490, 1969.
- [5] Harder, F. L. Jr, Kelson, I. K., Kishida, T., Kayen, R. "Preliminary Observations of the Fujinuma Dam Failure Following the March 11, 2011 Tohoku Offshore Earthquake, Japan", *Geotechnical Extreme Events Reconnaissance (GEER)*, Berkeley, California, 2011
- [6] Seed, B.H. "Earthquake-Resistant Design of Earth Dams", In: *First International Conference on Recent Advances in Geotechnical Earthquake Engineering & Soil Dynamics*, Rolla, Missouri, 1981.
- [7] Gazetas, G., Dakoulas, P. "Seismic analysis and design of rockfill dams: state-of-the-art", *Soil Dynamics and Earthquake Engineering*, 11, pp. 27–61, 1992. [https://doi.org/10.1016/0267-7261\(92\)90024-8](https://doi.org/10.1016/0267-7261(92)90024-8)
- [8] Mitchell, K.J. "Recent Developments in Ground Improvement for Mitigation of Seismic Risk to Existing Embankment Dams", In: *Geotechnical Earthquake Engineering and Soil Dynamics Congress IV*, Sacramento, California, 2008, [https://doi.org/10.1061/40975\(318\)98](https://doi.org/10.1061/40975(318)98)
- [9] Boulanger, W.R., Montgomery, J., Ziotopoulou, K. "Nonlinear Deformation Analyses of Liquefaction Effects on Embankment Dams", In: Ansal A., Sakr M. (eds) *Perspectives on Earthquake Geotechnical Engineering*. Geotechnical, Geological and Earthquake Engineering, vol 37, Springer, Cham, 2015, pp 247–283, https://doi.org/10.1007/978-3-319-10786-8_10
- [10] Testo del decreto-legge 29 marzo 2004, n. 79 (in *Gazzetta Ufficiale - serie generale - n. 75 del 30 marzo 2004*), coordinato con la legge di conversione 28 maggio 2004, n. 139, recante: "Disposizioni urgenti in materia di sicurezza di grandi dighe e di edifici istituzionali."
- [11] Ausilio, E., Dente, G., Zimmaro, P. "Geotechnical investigation and field performance of a zoned earth dam in Italy", In: *1st IMEKO TC-4 International Workshop on Metrology for Geotechnics*, Benevento, Italy, 2016, pp. 281–287.
- [12] Ausilio, E., Dente, G., Zimmaro, P. "Osservazioni sul monitoraggio geotecnico della diga di Farneto del Principe", (Considerations on the geotechnical monitoring of the Farneto del Principe dam) In: *Incontro Annuale dei Ricercatori di Geotecnica (IARG)*, Perugia, Italy, 2013.
- [13] Zimmaro, P., Stewart J.P. "Site-specific seismic hazard analysis for Calabrian dam site using regionally customized seismic source and ground motion models", *Soil Dynamics and Earthquake Engineering*, 94, pp. 179–192, <https://doi.org/10.1016/j.soildyn.2017.01.014>
- [14] Kim, J-T., Kim, D-S., Park, H-J., Kwon, H-K. "Estimation of dynamic material properties for fill dam: I. In-situ shear wave velocity profiles" *Journal of the Korean Geotechnical Society*, 25, pp. 69–85, 2009.
- [15] Park, D., Kishida, T. "Shear wave velocity profiles of fill dams", *Soil Dynamics and Earthquake Engineering*, 104, 250–258, 2017, <http://dx.doi.org/10.1016/j.soildyn.2017.10.013>
- [16] Regina, G., Cairo, R., Zimmaro, P. "Ground response analyses for a zoned earth dam site in Southern Italy", In: *7th Italian National Congress of Geotechnical Researchers (CNRIG2019)*, Lecco, Italy, 2019, pp. 148–154.
- [17] Zimmaro, P. "Seismic response of the Farneto del Principe dam in Italy using hazard-consistent and site-specific ground motions", PhD Dissertation, University Mediterranea, Reggio Calabria, 2015.
- [18] Cavallaro, A., Maugeri, M., Lo Presti, D.C., Pallara, O. "Characterising Shear Modulus and Damping from in Situ and Laboratory Tests for the Seismic Area of Catania", In: *2nd International Symposium on Pre-failure Deformation Characteristics of Geomaterials*, Torino, Italy, pp. 51–58, 1999.
- [19] Park, D., Kishida, T. "Shear modulus reduction and damping ratio curves for earth core materials of dams", *Canadian Geotechnical Journal*, 56, pp. 14–22, 2019, <https://doi.org/10.1139/cgj-2017-0529>
- [20] Vucetic, M., Dobry, R. "Effect of Soil Plasticity on Cyclic Response", *Journal of Geotechnical Engineering*, 117, pp. 89–107, 1991, [https://doi.org/10.1061/\(ASCE\)0733-9410\(1991\)117:1\(89\)](https://doi.org/10.1061/(ASCE)0733-9410(1991)117:1(89))
- [21] Mayne, W.P., Rix, J.G. "Correlations between shear wave velocity and cone tip resistance in natural clays", *Soils and Foundations*, 35(2), pp. 107–110, 1995, https://doi.org/10.3208/sandf1972.35.2_107
- [22] Hegazy, A.Y., Mayne W.P. "Statistical correlations between VS and cone penetration data for different soil types", In: *Proceedings of International Symposium on Cone Penetration Testing, CPT '95*, Linkoping, Sweden, Vol. 2, pp. 173–178, 1995
- [23] Piratheepan, P. "Estimating Shear-Wave Velocity from SPT and CPT Data", Master of Science Thesis, Clemson University, 2002.
- [24] Mayne, W.P. "In situ test calibrations for evaluating soil parameters" In: *Proceedings of Characterization and Engineering Properties of Natural Soils II*, Singapore, 2006.
- [25] Mayne, W.P. "Cone penetration testing state-of-practice", NCHRP Project 20-05 Topic 37-14, 2007.
- [26] Wair, R. B., DeJong, T.J., Shantz, T. "Guidelines for Estimation of Shear Wave Velocity Profiles", *Pacific Earthquake Engineering Research Center (PEER)*, Berkeley, California, Rep. 08, 2012.
- [27] Ohta, Y., Goto, N. "Empirical shear wave velocity equations in terms of characteristic soil indexes", *Earthquake Engineering Structural Dynamics*, 6: pp. 167–187, 1978, <https://doi.org/10.1002/eqe.4290060205>
- [28] Lee, SHH "Analysis of the multicollinearity of regression equations of shear wave velocities", *Soils and Foundations*, 32(1), pp. 205–214, 1992, <https://doi.org/10.3208/sandf1972.32.205>

- [29] Athanasopoulos, G.A. "Empirical Correlations V_{so} - N_{spt} For Soils Of Greece: A Comparative Study Of Reliability", *Soil Dynamics and Earthquake Engineering*, 15, 1995
- [30] Pitilakis, K., Raptakis, D., Lontzetidis, K., Tika-Vassilikou, Th, Jongmans, D. "Geotechnical and geophysical description of Euro-Seistests, using field, and laboratory tests and moderate strong ground motions", *Journal of Earthquake Engineering*, 3(3), pp. 381–409, 1999, <https://doi.org/10.1080/13632469909350352>
- [31] Jafari, MK. Shafiee, A., Ramzkhah, A. "Dynamic properties of the fine grained soils in south of Tehran", *Journal of Seismology and Earthquake Engineering*, 4 (1), pp. 25–35, 2002.
- [32] Pietrantonì, M., Tagliaferri, A., Petrangeli, M. "Valutazione dell'affidabilità delle prove SPT per la caratterizzazione sismica dei terreni" (Evaluation of the SPT test reliability in the seismic characterization of soils), *Rivista Italiana di Geotecnica*, 1, pp. 17-31, 2013.
- [33] Dakoulas, P., Gazetas, G. "A class of inhomogeneous shear models for seismic response of dams and embankments", *International Journal of Soil Dynamics and Earthquake Engineering*, 4, pp. 166-182, 1985, [https://doi.org/10.1016/0261-7277\(85\)90037-3](https://doi.org/10.1016/0261-7277(85)90037-3)
- [34] Gazetas, G. "Seismic response of earth dams: some recent developments", *Soil Dynamics and Earthquake Engineering*, 6, pp. 2-47, 1987.